Neurobiology of Disease

Apolipoprotein E4 Produced in GABAergic Interneurons Causes Learning and Memory Deficits in Mice

Johanna Knoferle,[1,2] Seo Yeon Yoon,[1] David Walker,[1] Laura Leung,[1,2] Anna K. Gillespie,[1,3] Leslie M. Tong,[1,3] Nga Bien-Ly,[1,2] and Yadong Huang[1,2,3,4,5]

[1]Gladstone Institute of Neurological Disease, San Francisco, California 94158, [2]Department of Neurology and [3]Biomedical Science Program, University of California, San Francisco, California 94143, [4]Gladstone Institute of Cardiovascular Disease, San Francisco, California 94158, and [5]Department of Pathology, University of California, San Francisco, California 94143

Apolipoprotein (apo) E4 is expressed in many types of brain cells, is associated with age-dependent decline of learning and memory in humans, and is the major genetic risk factor for AD. To determine whether the detrimental effects of apoE4 depend on its cellular sources, we generated human apoE knock-in mouse models in which the human *APOE* gene is conditionally deleted in astrocytes, neurons, or GABAergic interneurons. Here we report that deletion of apoE4 in astrocytes does not protect aged mice from apoE4-induced GABAergic interneuron loss and learning and memory deficits. In contrast, deletion of apoE4 in neurons does protect aged mice from both deficits. Furthermore, deletion of apoE4 in GABAergic interneurons is sufficient to gain similar protection. This study demonstrates a detrimental effect of endogenously produced apoE4 on GABAergic interneurons that leads to learning and memory deficits in mice and provides a novel target for drug development for AD related to apoE4.

Key words: **apoE; astrocyte; conditional knock-out mice; GABAergic interneuron; learning and memory**

Introduction

AD is the most common form of dementia in the elderly and is marked by progressive cognitive decline (Hardy and Selkoe, 2002; Perrin et al., 2009; Huang and Mucke, 2012). Epidemiology studies identified that the major known genetic risk factor for AD is apolipoprotein (apo) E4 (Farrer et al., 1997), which was recently confirmed by genome-wide association studies (GWAS; Shi et al., 2012; Lambert, 2013; Zhang et al., 2013). ApoE4 carriers account for 60–75% of all AD cases (Farrer et al., 1997), and apoE4 increases the risk of the disease and lowers the age of onset in a gene dose-dependent manner (Corder et al., 1993; Saunders et al., 1993; Strittmatter et al., 1993).

GWAS also identified apoE4 as the only significant gene associated with age-related cognitive decline in humans (De Jager et al., 2012; Keenan et al., 2012). Interestingly, a longitudinal study showed that age-related memory decline in nondemented apoE4 carriers diverged from that of nondemented noncarriers before the age of 60 (Caselli et al., 2009). These findings suggest that apoE4 has a detrimental effect on cognition before the typical signs of AD arise. Additionally, human apoE4 knock-in (KI) mice displayed age-dependent deficits in spatial learning and memory, which were associated with an age-dependent loss of GABAergic interneurons in the hilus of the hippocampus (Andrews-Zwilling et al., 2010; Leung et al., 2012). Importantly, optogenetically inhibiting hilar GABAergic interneuron activity led to learning and memory deficits, suggesting that impairing hilar GABAergic interneurons directly causes cognitive deficits (Andrews-Zwilling et al., 2012).

ApoE is expressed in various types of brain cells, implicating that apoE derived from different cellular sources might have distinct roles in physiological and pathophysiological pathways (Huang, 2010; Huang and Mucke, 2012; Mahley and Huang, 2012). The primary source of apoE in the brain is in astrocytes, where the expression of apoE is increased during aging (Huang, 2010). ApoE is also expressed in CNS neurons, mostly in response to stress and injury (Xu et al., 2006; Huang, 2010; Huang and Mucke, 2012). Interestingly, when transgenically expressed in neurons, apoE3 is excitoprotective, whereas apoE4 is not; however, when transgenically expressed in astrocytes, apoE3 and apoE4 are equally excitoprotective (Buttini et al., 2010). Thus, the cellular source of apoE may affect its physiological and pathophysiological activities.

To definitively determine the cellular source-specific effects of apoE4 on the development of learning and memory deficits, we generated human apoE knock-in mouse models in which the human *APOE* gene (*APOE*) was conditionally deleted in astrocytes, neurons, or GABAergic interneurons. Using these unique mouse models, we demonstrate a detrimental effect of endogenous-produced apoE4 on hilar GABAergic interneurons, leading to learning and memory deficits in aged mice.

Received June 4, 2014; revised Sept. 2, 2014; accepted Sept. 9, 2014.

Author contributions: J.K. and Y.H. designed research; J.K., S.Y.Y., D.W., L.L., A.K.G., L.M.T., N.B.-L., and Y.H. performed research; J.K., S.Y.Y., D.W., L.L., A.K.G., L.M.T., and Y.H. analyzed data; J.K. and Y.H. wrote the paper.

This work was supported in part by grants P01AG022074, 1RF1AG047655, and P30NS065780 from the National Institutes of Health; Grant Kn 1015/1-1 from the German Research Foundation; the S.D. Bechtel, Jr. Foundation; and the Hellman Foundation. We thank T. Michael Gill, Ravikumar Ponnusamy, and Iris Lo for assistance on behavioral tests; Gary Howard and Crystal Herron for editorial assistance; and Linda Turney for manuscript preparation.

The authors declare no competing financial interests.

Correspondence should be addressed to Dr. Yadong Huang, Gladstone Institute of Neurological Disease, University of California, San Francisco, CA 94158. E-mail: yhuang@gladstone.ucsf.edu.

DOI:10.1523/JNEUROSCI.2281-14.2014

 0270-6474/14/3414069-11$15.00/0

Materials and Methods

Animals. LoxP-floxed apoE knock-in (apoE-fKI) mice were generated as described previously (Bien-Ly et al., 2012). To generate mice with a conditional deletion of the human *APOE* gene, homozygous apoE3-fKI (apoE3/3) and apoE4-fKI (apoE4/4) mice were crossbred with GFAP-Cre transgenic mice [B6.Cg-Tg(GFAP-cre)8Gtm] (Bajenaru et al., 2002; Uhlmann et al., 2002), Synapsin 1-Cre (Syn-1-Cre) transgenic mice [B6.Cg-Tg(Syn1-cre)671Jxm/J] (Zhu et al., 2001), or Dlx-Cre transgenic mice [Tg(I12b-cre)] (Potter et al., 2009). These lines generated mice that were heterozygous for apoE3 or apoE4 and positive for GFAP-Cre, Syn-I-Cre, or Dlx-Cre. These mice were further crossbred with homozygous apoE3-fKI or apoE4-fKI mice to generate mice that were homozygous for apoE3 or apoE4 and positive for GFAP-Cre (apoE-fKI/GFAP-Cre), Syn-I-Cre (apoE-fKI/Syn-1-Cre), or Dlx-Cre (apoE-fKI/Dlx-Cre). Littermates that were negative for GFAP-Cre, Syn-I-Cre, or Dlx-Cre were used as controls. For generation of the apoE-fKI/Syn-I-Cre line, only female Syn-I-Cre mice were used for breeding purposes because germline recombination has been reported in the progeny of male Syn-I-Cre mice (Rempe et al., 2006). To characterize Cre-recombinase expression, we crossbred Syn-1-Cre and Dlx-Cre transgenic mice with a Cre-reporter mouse line [Gt(ROSA)26Sor$^{tm6(CAG-ZsGreen1)Hze}$] (Madisen et al., 2010). For tissue collection, mice were anesthetized with intraperitoneal injection of 375 mg/kg tribromoethanol and transcardially perfused for 1 min with 0.9% saline. Brains were harvested on ice. Right hemibrains were drop fixed for 48 h in 4% paraformaldehyde and subsequently cryoprotected in 30% sucrose, and left hemibrains were snap frozen on dry ice. For laser-capture microscopy, hemibrains were perfused, embedded in optimal cutting temperature (O.C.T.) Compound (Tissue Tek), and snap frozen on dry ice.

Morris water maze test. Due to the large sample sizes, there were three separate Morris water maze (MWM) test cohorts. Each cohort contained littermate controls. Since control mice of apoE3-fKI and apoE4-fKI showed no significant difference across three cohorts and the conclusion was the same if we used pooled data or data from individual cohorts, we presented the pooled data for easier and more relevant comparisons. The MWM was performed as described previously (Andrews-Zwilling et al., 2010; Leung et al., 2012). A platform (15 cm in diameter) was located in a water maze pool (diameter 122 cm) that was filled with opaque water (18–20°C). The platform was submerged 1.5 cm from the surface during the hidden platform sessions (Raber et al., 1998; Harris et al., 2003; Andrews-Zwilling et al., 2010) and marked with a black-and-white-striped mast (15 cm high) during the cued training sessions. The platform location was constant during the hidden platform session (northwest quadrant) and was altered between the remaining quadrants during the cued training sessions. Only female mice at 17 months of age (10–25 mice per group) were used. Mice were trained to locate the hidden platform (hidden days 1–5) in two daily sessions separated by at least 2.5 h. Each session consisted of two trials 15 min apart, each lasting 60 s. Entry points were changed semirandomly between trials, but were repeated in the same order each day. Escape latency is noted as the time taken to locate the hidden platform. Swim speed is defined as the path length to the platform divided by latency. In the probe trials 24, 72, and 120 h after the last hidden platform training, the performance of each mouse was monitored for 60 s with an EthoVision video-tracking system (Noldus Information Technology). For the probe trials, the hidden platform was removed, and the entry point remained constant at a 180° angle opposite from the original platform location. Performance in the probe trials was analyzed by comparing the percentage of time spent in the target quadrant to the average of percentage time spent in all other three quadrants. Visible platform tests were performed after the last probe trial and consisted of one trial/platform location. Visible platform locations were quadrants that were not used for hidden platform training. Time between visible platform trials was 2 h.

Immunohistochemistry. The entire hippocampi of PFA-fixed and cryoprotected hemibrains were cut continuously into coronal sections with a microtome (30 μm; Leica SM200R) and divided into subseries of every tenth section, yielding eight to nine hippocampal sections in each hemibrain (Ramos et al., 2006; Takahashi et al., 2010). For quantitative immunohistochemical analysis of GABAergic interneurons, one subseries of every tenth section was immunostained with rat anti-somatostatin (1:100 for DAB; Millipore) overnight at 4°C. Primary antibodies were detected with biotinylated rabbit anti-rat IgG (1:250; Vector Laboratories) for DAB staining (DAB peroxidase substrate kit; Vector Laboratories). Brain sections of each experiment were processed in parallel using the same batches of solutions to minimize variability in immunohistochemical labeling conditions. For each antibody, the specificity of the immune reaction was controlled by omitting the primary antibody. For immunofluorescence analysis, the following primary antibodies were incubated overnight at 4°C: polyclonal goat anti-apoE antibody (1:5000; Calbiochem), polyclonal rabbit anti-Cre antibody (1:5000; Novagen), monoclonal mouse anti- NeuN antibody (1:2000; Millipore), polyclonal rabbit anti- GFAP antibody (1:2000; DAKO), monoclonal mouse anti-GFAP (1:2000; Millipore), polyclonal rabbit anti-GABA antibody (1:1000; Sigma), polyclonal rabbit anti-somatostatin antibody (1:500; Bachem). The following secondary antibodies were incubated for 1 h at room temperature: donkey anti-goat Alexa 488, donkey anti-rabbit Alexa 488, donkey anti-rabbit Alexa 594, and donkey anti-mouse Alexa 594 (all 1:1000; Invitrogen). Stained sections were examined with an inverted fluorescence microscope (Keyence BZ9000) or with a confocal microscope (MC13; Leica SP5).

Quantitative analysis of immunostained sections. Hilar somatostatin-positive interneuron numbers were quantified by design-based stereology, which is founded on the assumption that cell numbers estimated from serial plane sections are representative of the entire hippocampus (West, 1993; Løkkegaard et al., 2001; Mouton et al., 2002). Somatostatin-positive interneurons in the hilus of the hippocampus were counted in every tenth serial coronal section throughout the rostrocaudal extend of the hippocampus by an investigator blinded to genotype and then multiplied by 2 (for both hemispheres) and by 10 (for every tenth serial section; Andrews-Zwilling et al., 2010; Leung et al., 2012). The hilus is described as the polymorphic nuclear region between the inner border of the granule cell layer of the dentate gyrus and an imaginary connection between the ends of its granule cell layer blades, with exclusion of the interposed layer of CA3 pyramidal neurons. Stained cells touching the granular layer or cells within the CA3 layer were excluded. Only cells with clear cell boundaries were counted, while very lightly stained cells or positive signals with irregular shapes were excluded.

Western blot analysis. For protein lysate preparation, frozen hemibrains (five per group) were thawed slowly on ice and dissected to isolate the hippocampus and the cortex. Hippocampus and cortex were separately homogenized in ice-cold, high-detergent lysis buffer (10× w/v, 50 mM Tris, pH7.4, 150 mM NaCl, 2% NP-40, 0.5% sodium deoxycholate, 4% SDS, and protease and phosphatase inhibitor cocktails) and centrifuged at 30,000 rpm for 30 min (Optima TLX Ultracentrifuge; Beckman Coulter; Harris et al., 2003; Bien-Ly et al., 2012). The supernatant was collected, and total protein concentration was assessed with a bicinchoninic acid protein assay kit (Thermo Scientific). Relative apoE and tubulin levels were analyzed by Western blot. Briefly, 15 μg of protein lysates were loaded onto 4–12% Bis-Tris SDS-PAGE gels (Novex) and separated by electrophoresis. Proteins were transferred onto nitrocellulose membranes at 18 V for 60 min (Trans-Blot Turbo Transfer System; Bio-Rad). Nonspecific binding sites were blocked with blocking buffer (LI-COR Biosciences) for 1 h. Membranes were incubated with polyclonal goat anti-apoE antibody (1:5000; Calbiochem) and monoclonal mouse anti-GAPDH antibody (1:10,000; Millipore Bioscience Research Reagents) overnight at 4°C. Secondary antibodies, anti-goat antibody coupled to an 800-nm fluorophore (LI-COR Biosciences) for detecting apoE and anti-mouse antibody coupled to an 680 nm fluorophore (LI-COR Biosciences) for detecting GAPDH, were incubated for 1 h at room temperature in the dark. Resulting bands were detected with the Odyssey Imager (LI-COR Biosciences), and the fluorescence intensity of bands representing apoE was quantified as a ratio to bands representing GAPDH (ImageJ).

Laser capture microscopy and PCR analysis. For laser capture microscopy (LCM), frozen hemibrains embedded in O.C.T. compound were cut into 5 μm coronal sections with a cryostat (Leica) and mounted on uncharged glass slides (Fisher) treated with poly-L-lysine (0.1% w/v;

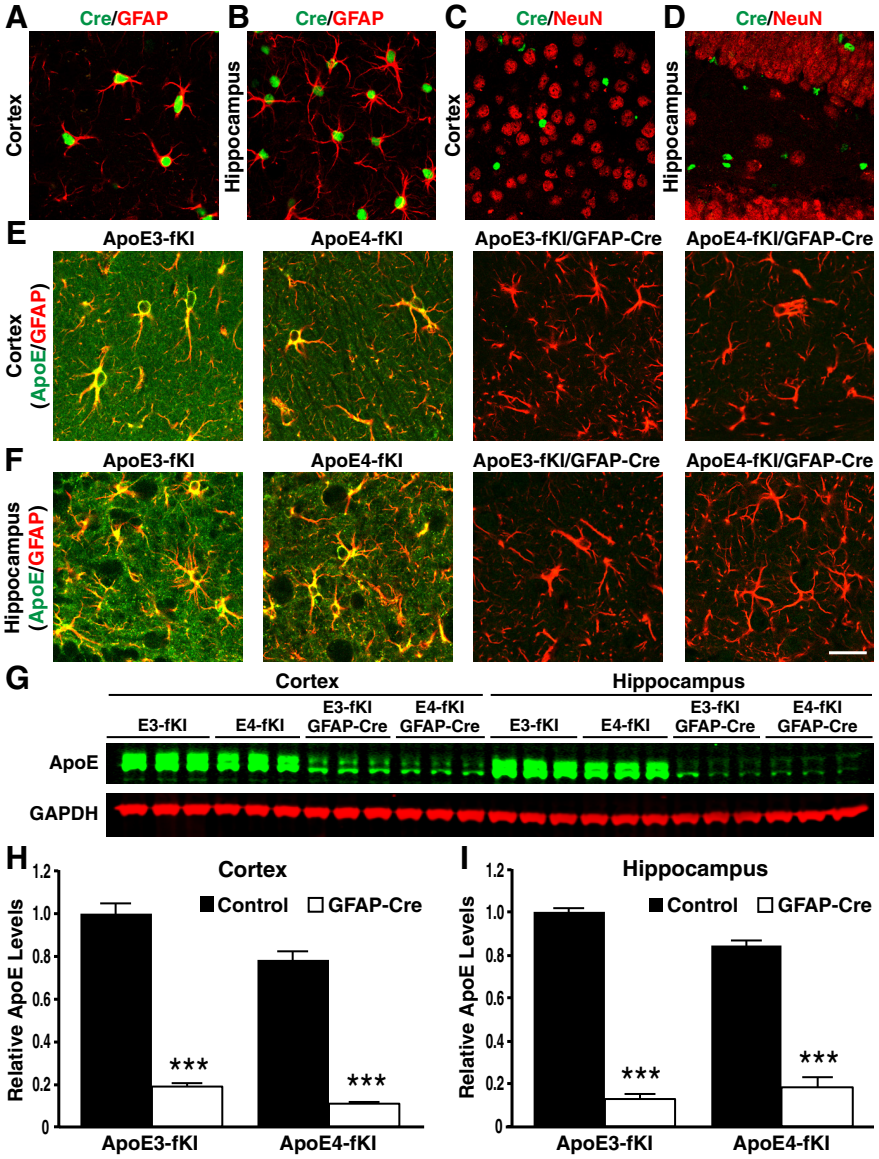

Figure 1. Generation and characterization of apoE-fKI/GFAP-Cre mice. ***A***, ***B***, Representative images of fluorescent immunostaining with anti-Cre recombinase (green) and anti-GFAP (red) in the cortex (***A***) and hippocampus (***B***) of apoE-fKI/GFAP-Cre mice. ***C***, ***D***, Neurons immunostained with anti-NeuN (red) did not express Cre-recombinase in the cortex (***C***) or hippocampus (***D***) of apoE-fKI/GFAP-Cre mice. ***E***, ***F***, Anti-apoE (green) and anti-GFAP (red) double immunostaining revealed that apoE expression was dramatically decreased in cortical (***E***) and hippocampal (***F***) astrocytes in apoE3-fKI/GFAP-Cre and apoE4-fKI/GFAP-Cre mice. ***G***, Representative fluorescent Western blot of apoE (green) and GAPDH (red) in cortical and hippocampal lysates of 17-month-old female mice with different genotypes. ***H***, ***I***, Quantification of apoE protein levels relative to GAPDH in cortical (***H***) and hippocampal lysates (***I***) of 17-month-old mice ($n = 5$/genotype). ApoE levels in apoE3-fKI mice were normalized to 1, and apoE levels in other groups of mice were presented relative to those in apoE3-fKI mice. $^{***}p < 0.001$ (*t* test). Scale bar, 50 μm.

Sigma) for 30 min at room temperature for better adherence of brain sections. Sections were fixed in ice-cold 70% ethanol for 10 min, briefly washed in PBS, followed by a 30-min incubation with monoclonal mouse anti-NeuN antibody (1:100; Millipore) or polyclonal rabbit anti-GABA antibody (1:50; Sigma). Secondary antibodies were donkey anti-mouse Alexa 488 or donkey anti-rabbit Alexa 488 (both 1:500, 30 min). Sections were dehydrated with an ethanol gradient and subjected to LCM immediately. Forty to sixty NeuN-positive neuronal nuclei in the granule cell layer of the dentate gyrus or the same number of GABAergic interneurons in the hilus of the dentate gyrus were dissected using LCM (PALM System; Leica). Dissected material was captured using special microfuge tubes with adhesive caps (AdhesiveCap, 200 μl; Zeiss). Genomic DNA was isolated by incubation with 15 μl of a 50 mM NaOH solution for 30 min at 95°C. We performed PCRs with primer pairs binding upstream of the 5′ loxP site and downstream of the 3′ loxP site (primers 1 and 3) or upstream and downstream of the 5′ loxP site (primers 1 and 2; (Figs. 3*J*, 5*J*). PCR products were analyzed by agarose gel electrophoresis.

Statistical analysis. All values are expressed as mean ± SEM. Statistical analyses were performed with GraphPad Prism version 5.0 software. MWM data were analyzed and compared by repeated-measures one-way ANOVA and Bonferroni *post hoc* test for the hidden training days and by one-way ANOVA and Bonferroni *post hoc* test for the probe trials. Statistical significance of histochemical quantification and immunoblotting was tested by *t* test. A *p* value of <0.05 was considered to be statistically significant. Statistical values are denoted as follows: $^{*}p < 0.05$, $^{**}p < 0.01$, $^{***}p < 0.001$.

Results

Deletion of apoE4 in astrocytes does not prevent learning and memory deficits in aged mice

Our laboratory previously generated mice expressing human apoE3 or apoE4 in place of mouse apoE, in which the knocked-in human *APOE3* or *APOE4* gene was flanked with a pair of LoxP sites, allowing for excision of the *APOE* gene in the presence of Cre-recombinase (Bien-Ly et al., 2012). We crossbred "floxed" KI mouse lines homozygous for apoE3 or apoE4 (referred to as apoE3-fKI and apoE4-fKI) with mice expressing Cre-recombinase under control of a GFAP promoter [B6.Cg-Tg(GFAP-cre) 8Gtm] (Bajenaru et al., 2002; Uhlmann et al., 2002). The progeny included homozygous apoE3-fKI and apoE4-fKI mice either negative (controls) or positive for GFAP-Cre (apoE3-fKI/GFAP-Cre and apoE4-fKI/GFAP-Cre). By immunostaining brain sections from apoE-fKI/GFAP-Cre mice with a Cre-specific antibody, we observed Cre expression throughout the cortex and hippocampus (Fig. 1*A–D*). We then confirmed expression of Cre in cortical and hippocampal astrocytes by coimmunostaining with GFAP antibody (Fig. 1*A*,*B*). Cre recombinase was not expressed in NeuN-positive neurons in the cortex and hippocampus of Cre-positive mice (Fig. 1*C*,*D*).

By anti-apoE and anti-GFAP double immunostaining, we detected high levels of apoE in astrocytes and neuropils in the cortex and hippocampus of apoE3-fKI and apoE4-fKI mice (Fig. 1*E*,*F*, left). ApoE levels were dramatically decreased in the cortex and hippocampus of apoE3-fKI/GFAP-Cre and apoE4-fKI/GFAP-Cre mice (Fig. 1*E*,*F*, right). To quantitatively determine reduced apoE expression in cerebral subregions of apoE-fKI/GFAP-Cre mice, we used Western blots to analyze apoE in the cortical and hippocampal lysates of 17-month-old female mice that had been tested in the MWM. We observed lower apoE protein levels in apoE4-fKI than in apoE3-fKI mice, similar to a previous report

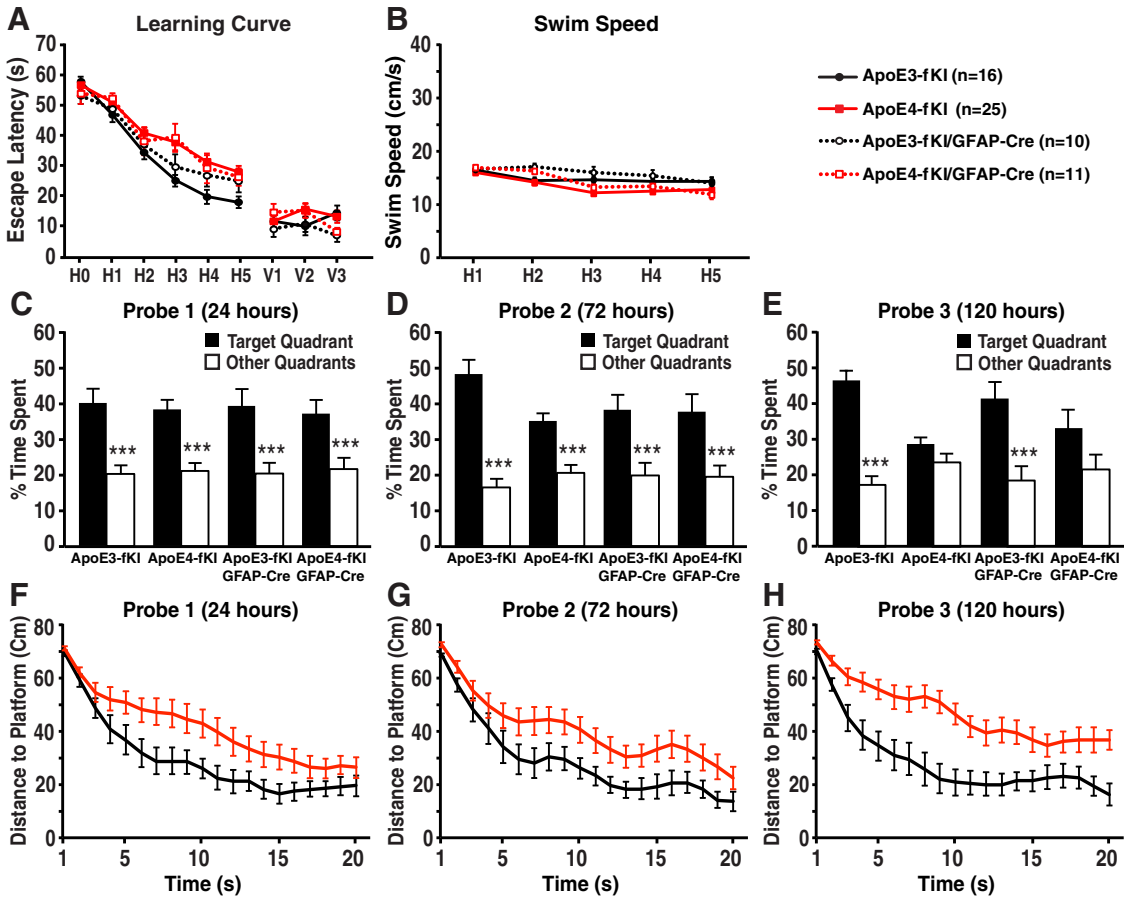

Figure 2. Deletion of apoE4 in astrocytes did not prevent the development of spatial learning and memory deficits in aged mice. ***A***, Seventeen-month-old female apoE3-fKI, apoE4-fKI, apoE3-fKI/GFAP-Cre, and apoE4-fKI/GFAP-Cre mice were tested in the MWM. Points represent averages of daily trials. H, hidden platform day (2 trials per session, 2 sessions per day); H0, first trial on H1; V, visible platform day (1 trial per platform location, 3 sessions per day). Escape latency (*y*-axis) indicates time to reach the target. On the hidden platform days, latencies were analyzed and compared by repeated-measures ANOVA and Bonferroni *post hoc* test. ApoE4-fKI mice learned more slowly than apoE3-fKI mice ($p < 0.01$). ApoE4-fKI/GFAP-Cre mice learned significantly slower than apoE3-fKI mice ($p < 0.05$). There was no significant difference between apoE4-fKI and apoE4-fKI/GFAP-Cre mice. ***B***, Swim speed was similar among the four groups of mice. ***C–E***, Probe 1, 2, and 3 trials were performed 24, 72, and 120 h, respectively, after the last day of hidden platform training. Percentage time spent in the target quadrant versus the average percentage time spent in the other three quadrants was compared for each group of mice; $^{***}p < 0.001$ (one-way ANOVA and Bonferroni *post hoc* test). ***F–H***, Average distance to target platform (in centimeters) for the first 20 s of probe trials 1 (***F***), 2 (***G***), and 3 (***H***). (Repeated measures two-way ANOVA, apoE3-fKI vs apoE4-fKI: probe 1, $p < 0.05$; probe 2, $p < 0.05$; probe 3, $p < 0.001$.)

(Bien-Ly et al., 2012). After deleting *APOE* from astrocytes of apoE3-fKI/GFAP-Cre and apoE4-fKI/GFAP-Cre mice, apoE protein levels were reduced to ~20% of those seen in the cortex and hippocampus of apoE3-fKI and apoE4-fKI mice (Fig. 1*G–I*). These data indicate that apoE expression is abolished by GFAP-Cre in astrocytes in the cortex and hippocampus of apoE-fKI/GFAP-Cre mice and, furthermore, that the remaining low levels of apoE might be expressed in other brain cells.

Next, we tested whether deleting apoE in astrocytes would affect spatial learning and memory with the MWM test. Seventeen-month-old female apoE3-fKI mice quickly learned to find the hidden platform, whereas the escape latencies of age-matched female apoE4-fKI mice were significantly longer (Fig. 2*A*), suggesting that the apoE4-fKI mice had spatial learning deficits. Deleting apoE4 in astrocytes did not improve spatial learning in apoE4-fKI/GFAP-Cre mice (Fig. 2*A*), suggesting that astrocytic apoE4 does not significantly contribute to learning deficits. Interestingly, when apoE3 was deleted in astrocytes, apoE3-fKI/GFAP-Cre mice displayed decreased learning, although not statistically significant, compared with apoE3-fKI mice (Fig. 2*A*). Among the four groups of mice, visible trial performance and swim speeds were not significantly different (Fig. 2*A*,*B*). In all three probe trials (24, 72, and 120 h after hidden platform training) for spatial memory test, apoE3-fKI mice spent significantly more time in the target quadrant than other quadrants, indicating that the mice remembered the platform location (Fig. 2*C–E*). Conversely, although apoE4-fKI mice performed equally well as apoE3-fKI mice in the first and second probe trial, apoE4-KI mice did not recall the platform quadrant in the third probe trial, suggesting that their memory was impaired (Fig. 2*C–E*). To further determine whether apoE4-fKI mice had true memory impairment or extinction, we analyzed the traveling distance to the platform during the first 20 s of each probe trial (Gallagher et al., 1993; Maei et al., 2009). In this more stringent test, apoE4-fKI mice had significantly longer distance to platform for all three probe trials (Fig. 2*F–H*), indicating that their memory was truly impaired. Importantly, deleting apoE3 or apoE4 in astrocytes did not significantly alter the memory performance of apoE3-fKI/GFAP-Cre and apoE4-fKI/GFAP-Cre mice as compared with their corresponding controls (apoE3-fKI and apoE4-fKI mice, respectively; Fig. 2*C–E*). These data indicate that deletion of

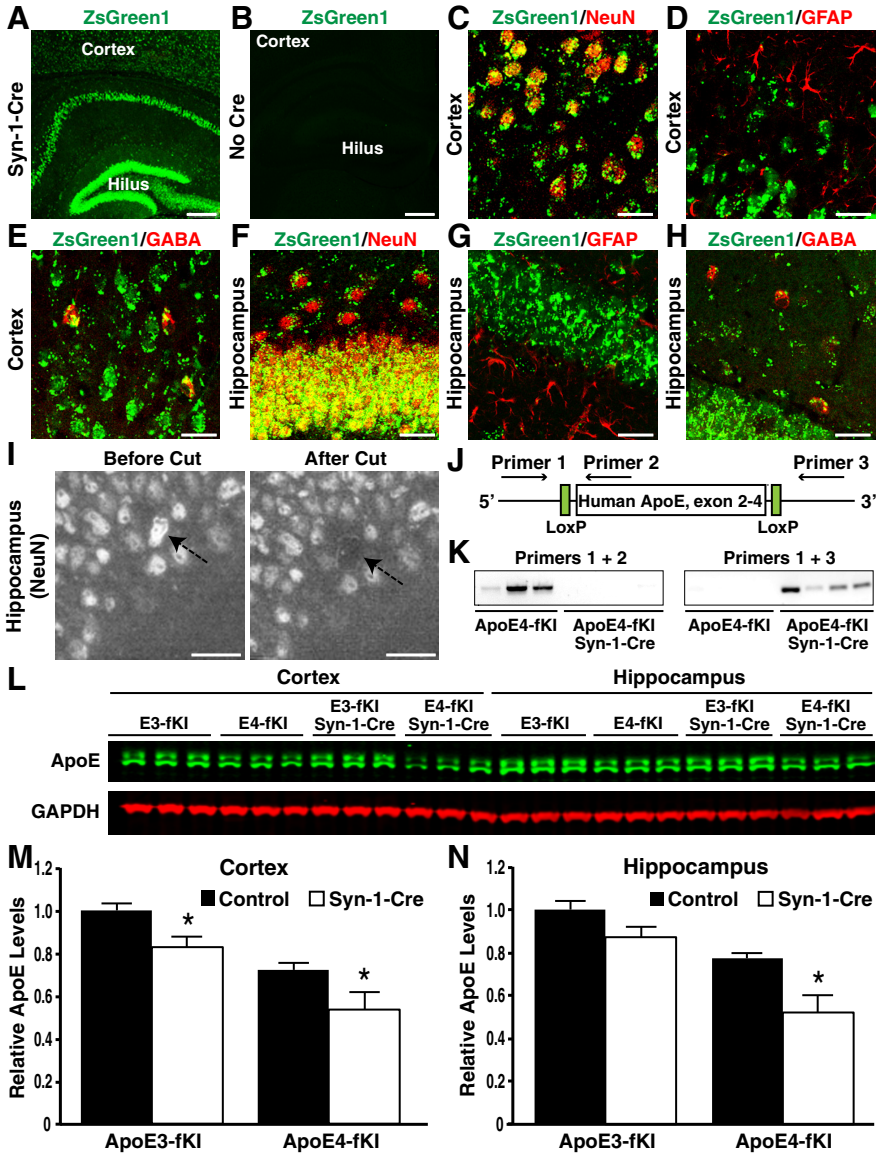

Figure 3. Generation and characterization of apoE-fKI/Syn-1-Cre mice. ***A***, ***B***, Expression of ZsGreen1 (green) in the cortex and hippocampus of Syn-1-Cre-positive (***A***) and -negative (***B***) ZsGreen1 reporter mice. Scale bars: 250 μm. ***C–H***, ZsGreen1 was expressed in NeuN-positive neurons (***C***, ***F***) and GABA-positive inhibitory interneurons (***E***, ***H***), but not in GFAP-positive astrocytes (***D***, ***G***) in the cortex and hippocampus of Syn-1-Cre-positive apoE-fKI mice. Scale bars: 30 μm. ***I***, Images of the dentate granular cell layer before and after laser capture. Neuronal nuclei were identified by anti-NeuN immunostaining. Arrows indicate the cell before and after laser capture. Scale bars: 30 μm. ***J***, Schematic of primers and their binding sites on the human *APOE* gene. ***K***, PCR with primers 1 and 2 resulted in an amplified product in samples of apoE4-fKI mice, but not in samples of apoE4-fKI/Syn-1-Cre mice (left). PCR with primers 1 and 3 resulted in an amplified product in samples of apoE4-fKI/Syn-1-Cre mice, but not in samples of apoE4-fKI mice (right). Fifty nuclei per sample were used. ***L***, Representative fluorescent Western blot of apoE (green) and GAPDH (red) in cortical and hippocampal lysates of 17-month-old female mice with different genotypes. ***M***, ***N***, Quantification of apoE protein levels relative to GAPDH protein levels in cortical (***M***) and hippocampal lysates (***N***) of 17-month-old mice ($n = 5$ per genotype). ApoE levels in apoE3-fKI mice were normalized to 1, and apoE levels in other groups of mice were presented relative to those in apoE3-fKI mice. $^*p < 0.05$ (*t* test).

apoE4 in astrocytes does not prevent the development of learning and memory deficits in aged mice.

Deletion of apoE4 in neurons prevents learning and memory deficits in aged mice

To investigate the effects of deleting apoE in neurons on neuronal and behavioral deficits, we crossbred apoE3-fKI and apoE4-fKI mice with mice expressing Cre recombinase under control of a neuron-specific Synapsin-1 promoter [B6.Cg-Tg(Syn1-cre)671Jxm/J] (referred to as Syn-1-Cre; Zhu et al., 2001). The progeny included homozygous apoE3-fKI and apoE4-fKI control mice, as well as apoE3-fKI/Syn-1-Cre and apoE4-fKI/Syn-1-Cre mice. To analyze the Cre-expression pattern, we also crossbred Syn-1-Cre mice with a Cre-reporter mouse line with a floxed stop codon in front of ZsGreen1, an optimized enhanced EGFP [Gt(ROSA)26Sor$^{tm6(CAG-ZsGreen1)Hze}$] (Madisen et al., 2010). Upon Cre recombination, the stop codon is deleted, and ZsGreen1 is expressed specifically in Cre-positive cells. As expected, in mice positive for Syn-1-Cre and the reporter gene, we observed strong ZsGreen1 expression throughout the entire brain, including the hippocampus and cortex (Fig. 3*A*). ZsGreen1 expression did not leak in mice negative for Syn-1-Cre and positive for the reporter gene (Fig. 3*B*). We then confirmed ZsGreen1 expression in the cortex and hippocampus by immunostaining with a pan-neuronal marker, NeuN, and a GABAergic inhibitory interneuron selective marker, GABA (Fig. 3*C*,*E*,*F*,*H*). ZsGreen1 was not expressed in GFAP-positive astrocytes (Fig. 3*D*,*G*).

To confirm the deletion of apoE in Syn-1-Cre-positive neurons, we isolated NeuN-positive nuclei in the dentate gyrus by LCM and genotyped the isolated genomic DNA (gDNA) for the human *APOE* gene (Fig. 3*I*). For PCR amplification of the *APOE* gene, we used primer pairs with binding sites upstream of the 5′ loxP site and downstream of the 3′ lox P site (primers 1 and 3) or upstream and downstream of the 5′ loxP site (primers 1 and 2; Fig. 3*J*). When Syn-1-Cre was expressed, a PCR product was not amplified with primers 1 and 2, but was with primers 1 and 3, indicating the deletion of the human *APOE* gene (Fig. 3*K*). In contrast, in the absence of Syn-1-Cre expression, a PCR product was amplified from reactions with primers 1 and 2, but not with primers 1 and 3 (Fig. 3*K*). These data further support the conditional deletion of floxed *APOE* in neurons of Syn-1-Cre-positive mice.

We also analyzed the levels of apoE in the cortical and hippocampal lysates from different mice by Western blotting (Fig. 3*L*). In the cortex, deleting *APOE* in neurons reduced apoE levels by ~20% in both apoE3-fKI/Syn-1-Cre and apoE4-fKI/Syn-1-Cre mice (Fig. 3*M*). This suggests that neuronal apoE contributes ~20% of total apoE protein levels in the cortex. This is consistent with the observation that the remaining apoE was ~20% of the total apoE protein levels when *APOE* was deleted in astrocytes (Fig. 1*H*). In the hippocampus, deleting *APOE* in neurons reduced apoE protein levels by ~10% in apoE3-fKI/Syn-1-Cre mice and by ~30% in apoE4-fKI/Syn-1-Cre mice (Fig. 3*N*).

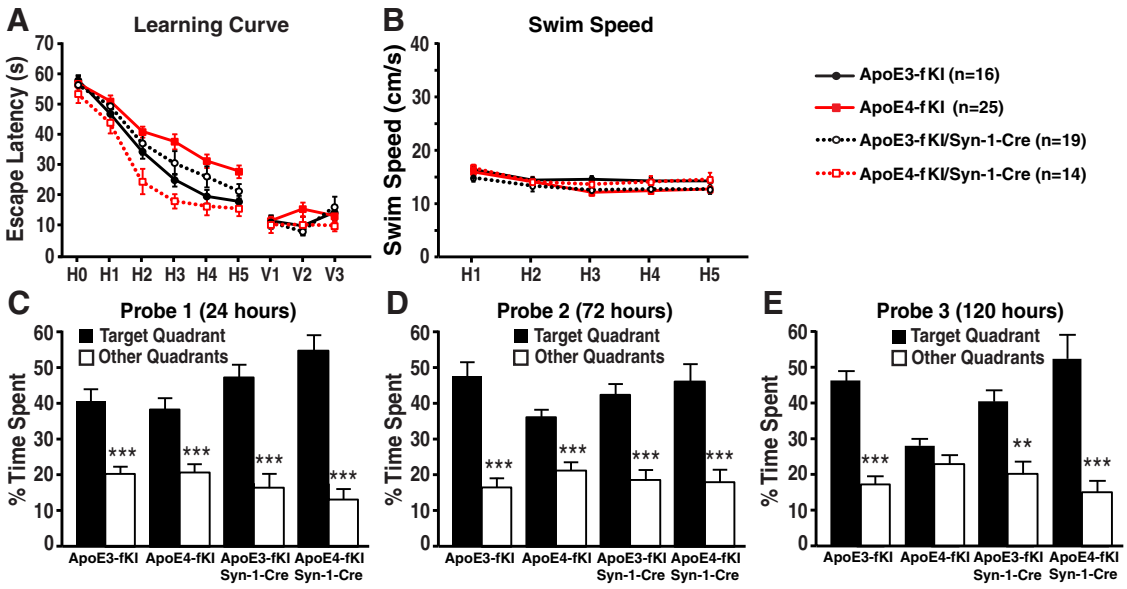

Figure 4. Deletion of apoE4 in neurons prevented the development of spatial learning and memory deficits in aged mice. ***A***, Seventeen-month-old female apoE3-fKI, apoE4-fKI, apoE3-fKI/Syn-1-Cre, and apoE4-fKI/Syn-1-Cre mice were tested in the MWM. Points represent averages of daily trials. H, hidden platform day (2 trials per session, 2 sessions per day); H0, first trial on H1; V, visible platform day (1 trial per platform location, 3 sessions per day). Escape latency (*y*-axis) indicates time to reach the target. In the hidden platform days, latencies of all groups of mice were analyzed and compared by repeated-measures ANOVA and Bonferroni *post hoc* test. ApoE4-fKI mice learned significantly slower than apoE3-fKI mice ($p < 0.01$). ApoE4-fKI/Syn-1-Cre mice learned as well as apoE3-fKI mice ($p > 0.05$), which was significantly faster than apoE4-fKI mice ($p < 0.001$). There was no significant difference between apoE3-fKI and apoE3-fKI/Syn-1-Cre mice. ***B***, Swim speed was similar among the four groups of mice. ***C–E***, Probe 1, 2, and 3 trials were performed 24, 72, and 120 h, respectively, after the last day of hidden platform training. Percentage time spent in the target quadrant and the average percentage time spent in other three quadrants were compared for each group of mice. $^{**}p < 0.01$, $^{***}p < 0.001$ (one-way ANOVA and Bonferroni *post hoc* test).

In the MWM test, deleting apoE4 in neurons completely prevented the spatial learning deficits in aged apoE4-fKI/Syn-1-Cre mice, as compared with apoE4-fKI mice (Fig. 4*A*). Again, we observed decreased learning, although not statically significant, when apoE3 was deleted in neurons in apoE3-fKI/Syn-1-Cre mice, as compared with apoE3-fKI mice (Fig. 4*A*). We did not see a difference in visible trial performance and swim speeds between all four groups of mice (Fig. 4*A*,*B*). In probe trials (Fig. 4*C–E*), deleting apoE4 in neurons completely prevented the development of memory impairment, making the performance of apoE4-fKI/Syn-1-Cre mice similar to that of apoE3-fKI mice (Fig. 4*E*). Additionally, deleting apoE3 in neurons did not significantly alter memory performance in all three probe trials (Fig. 4*C–E*). These results indicate that deletion of apoE4 in neurons prevents the development of learning and memory deficits in aged mice.

Deleting apoE4 in GABAergic interneurons is sufficient to prevent learning and memory deficits in aged mice

We previously reported that apoE4-induced dysfunction or loss of GABAergic interneurons in the hilus of the hippocampus correlates with the extent of learning and memory deficits in apoE4-KI mice (Andrews-Zwilling et al., 2010; Leung et al., 2012). We then asked whether deleting apoE4 only in GABAergic interneurons would be sufficient to prevent aged apoE4-fKI mice from developing learning and memory deficits. To generate mice with a conditional deletion of *APOE* in GABAergic interneurons, we crossbred apoE3-fKI and apoE4-fKI mice with Dlx-I12b-Cre mice expressing Cre recombinase under the control of an enhancer specific for forebrain GABAergic interneurons (referred to as Dlx-Cre mice) (Potter et al., 2009). The progeny included homozygous apoE3-fKI and apoE4-fKI control mice and apoE3-fKI/Dlx-Cre and apoE4-fKI/Dlx-Cre mice. We analyzed the Cre expression pattern of Dlx-Cre-positive mice by crossbreeding them with the ZsGreen1 reporter line, as we described for the Syn-1-Cre mouse line. In ZsGreen1-positive mice, we confirmed Cre expression by strong ZsGreen1 expression throughout the entire brain, including the cortex and hippocampus, and there was no leaking ZsGreen1 expression in the absence of Dlx-Cre (Fig. 5*A*,*B*). Moreover, ZsGreen1 was specifically expressed in GABAergic inhibitory interneurons in the cortex and hippocampus, as determined by immunostaining with anti-GABA and anti-somatostatin (Fig. 5*C–F*). To confirm the deletion of *APOE* in GABAergic interneurons, we isolated gDNA from laser-capture, microdissected GABA-positive hilar interneurons in apoE-fKI/Dlx-Cre mice (Fig. 5*I*). To probe for deletion of *APOE*, we used the same PCR primer pairs (Fig. 5*J*) as described above. We did not detect an amplified PCR product for reactions with primers 1 and 2 in samples from apoE-fKI/Dlx-Cre mice, but did for reactions with primers 1 and 3 (Fig. 5*K*). In contrast, in samples from Dlx-Cre-negative apoE-fKI mice, we obtained an amplified PCR product from reactions with primers 1 and 2 but not with primers 1 and 3 (Fig. 5*K*). These data further support the conditional deletion of floxed *APOE* in apoE-fKI/Dlx-Cre mice. In line with this conclusion, immunostaining for apoE revealed the presence of apoE protein in GABA-positive hilar interneurons in aged apoE4-fKI mice, but not in apoE4-fKI/Dlx-Cre mice (Fig. 5*G*,*H*). We then analyzed apoE levels in the cortical and hippocampal lysates from 17-month-old female mice by Western blotting (Fig. 5*L*). Deleting *APOE* from GABAergic interneurons reduced apoE levels by ~20% in the cortex and hippocampus of apoE3-fKI/Dlx-Cre mice and by ~30% in the cortex and hippocampus of apoE4-fKI/Dlx-Cre mice (Fig. 5*M*,*N*). Thus, GABAergic neurons express significant amounts of apoE at least in aged mice.

In the MWM test, deletion of apoE4 in GABAergic interneurons completely prevented spatial learning deficits in aged apoE4-fKI/Dlx-Cre mice as compared with apoE4-fKI mice (Fig.

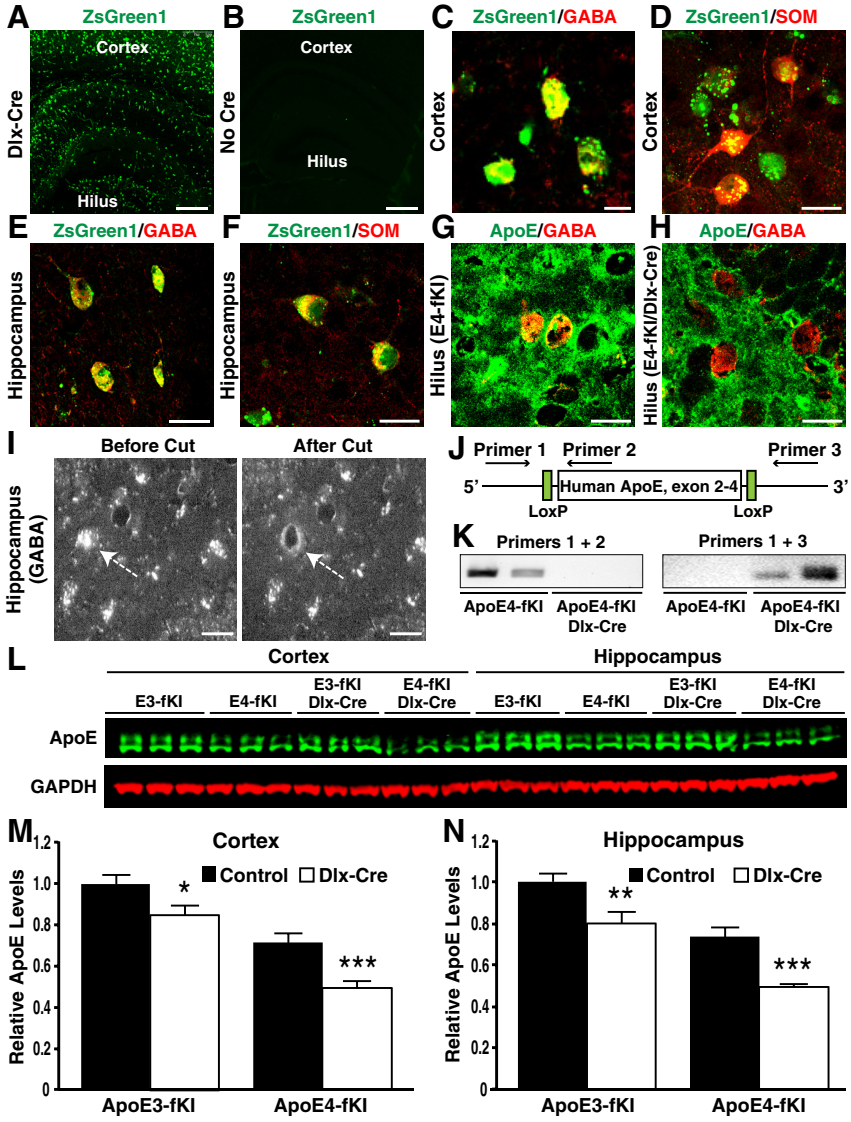

Figure 5. Generation and characterization of apoE-fKI/Dlx-Cre mice. ***A***, ***B***, Expression of ZsGreen1 (green) in the cortex and hippocampus of Dlx-Cre-positive (***A***) and -negative (***B***) ZsGreen1 reporter mice. Scale bars: 250 μm. ***C–F***, ZsGreen1 was expressed in GABA-positive (***C***, ***E***) and somatostatin (SOM)-positive (***D***, ***F***) inhibitory interneurons in the cortex and hippocampus of Dlx-Cre-positive apoE-fKI mice. Scale bars: 15 μm. ***G***, ***H***, Anti-apoE immunostaining revealed the presence of apoE protein in GABA-positive hilar interneurons in aged apoE4-fKI mice (***G***), but not in apoE4-fKI/Dlx-Cre mice (***H***). Scale bars: 15 μm. ***I***, Images of GABA-positive hilar interneurons before and after laser capture. Inhibitory interneuron were identified by anti-GABA immunostaining. Arrows indicate the cell before and after laser capture. Scale bars: 15 μm. ***J***, Schematic of primers and their binding sites on the human *APOE* gene. ***K***, PCR with primers 1 and 2 resulted in an amplified product in samples of apoE4-fKI mice, but not in samples of apoE4-fKI/Dlx-Cre mice (left). PCR with primers 1 and 3 resulted in an amplified product in samples of apoE4-fKI/Dlx-Cre mice, but not in samples of apoE4-fKI mice (right). Fifty nuclei per sample were used. ***L***, Representative fluorescent Western blot of apoE (green) and GAPDH (red) in cortical and hippocampal lysates of 17-month-old female mice with different genotypes. ***M***, ***N***, Quantification of apoE protein levels relative to GAPDH protein levels in cortical (***M***) and hippocampal lysates (***N***) of 17-month-old mice ($n = 5$ per genotype). For both the cortex and the hippocampus, the apoE level in apoE3-fKI mice was normalized to 1, and apoE levels in other groups of mice were presented relative to those in apoE3-fKI mice. *$p < 0.05$, **$p < 0.01$, ***$p < 0.001$ (*t* test).

6*A*). We actually found that the learning curve of apoE4-fKI/Dlx-Cre mice was identical to that of apoE3-fKI mice and that deleting apoE3 in GABAergic interneurons did not significantly alter learning performance. Visible trial performance and swim speed were not significantly different among all four groups of mice (Fig. 6*A*,*B*). In probe trials (Fig. 6*C–E*), deleting apoE4 from GABAergic interneurons completely prevented the development of memory impairment, making the performance of apoE4-fKI/Dlx-Cre mice comparable to that of apoE3-fKI mice (Fig. 6*E*). Conversely, deleting apoE3 from neurons did not significantly alter memory performance in all three probe trials (Fig. 6*C–E*). Thus, deleting apoE4 in GABAergic interneurons is sufficient to prevent learning and memory deficits in aged mice.

Deleting apoE4 in all neurons or GABAergic interneurons abolishes the detrimental effect of apoE4 on somatostatin-positive hilar interneurons in aged mice

We previously reported that apoE4-induced dysfunction or loss of GABAergic interneurons, especially somatostatin-positive interneurons, in the hilus of the hippocampus correlates with the extent of learning and memory deficits in apoE4-KI mice (Andrews-Zwilling et al., 2010; Leung et al., 2012). To determine the effect of the cellular source of apoE4 on somatostatin-positive hilar interneurons, we quantified the numbers of these cells in the hippocampal hilus of apoE3-fKI or apoE4-fKI mice without or with deletion of *APOE* in astrocytes, neurons, or GABAergic interneurons from mice subjected to the MWM test. Similar to previous reports (Andrews-Zwilling et al., 2010; Leung et al., 2012), we found that apoE4-fKI mice had 30% fewer somatostatin-positive hilar interneurons than apoE3-fKI mice (Fig. 7*A–D*). Additionally, deleting apoE4 in all neurons (apoE4-fKI/Syn-1-Cre) or in GABAergic interneurons alone (apoE4-fKI/Dlx-Cre) completely eliminated the detrimental effect of apoE4 on somatostatin-positive hilar interneurons, bringing their numbers up to the levels of apoE3-fKI mice (Fig. 7*A–D*). In sharp contrast, deleting apoE4 in astrocytes (apoE4-fKI/GAFP-Cre) could not prevent the loss of hilar somatostatin-positive interneurons (Fig. 7*A*,*B*). Moreover, deleting apoE3 from any of the three types of cells did not alter the numbers of hilar somatostatin-positive interneurons as compared with apoE3-fKI mice (Fig. 7*A–D*). These data indicate a detrimental effect of endogenously produced apoE4 on GABAergic interneurons.

Discussion

Our studies demonstrate that the cellular source of apoE4 determines the development of hilar GABAergic interneuron impairment and cognitive deficits in aged mice. Deleting apoE4 in astrocytes does not protect aged mice from hilar interneuron loss or impairment of spatial learning and memory. In contrast, deleting apoE4 in neurons protects aged mice from both deficits, an effect that is paralleled by deleting apoE4 in GABAergic interneurons.

In our study, we examined novel human apoE knock-in mouse models that allow for cell type-specific deletion of apoE expression, with physiological expression of apoE in the remaining types of cells in the brain. This is especially important as we

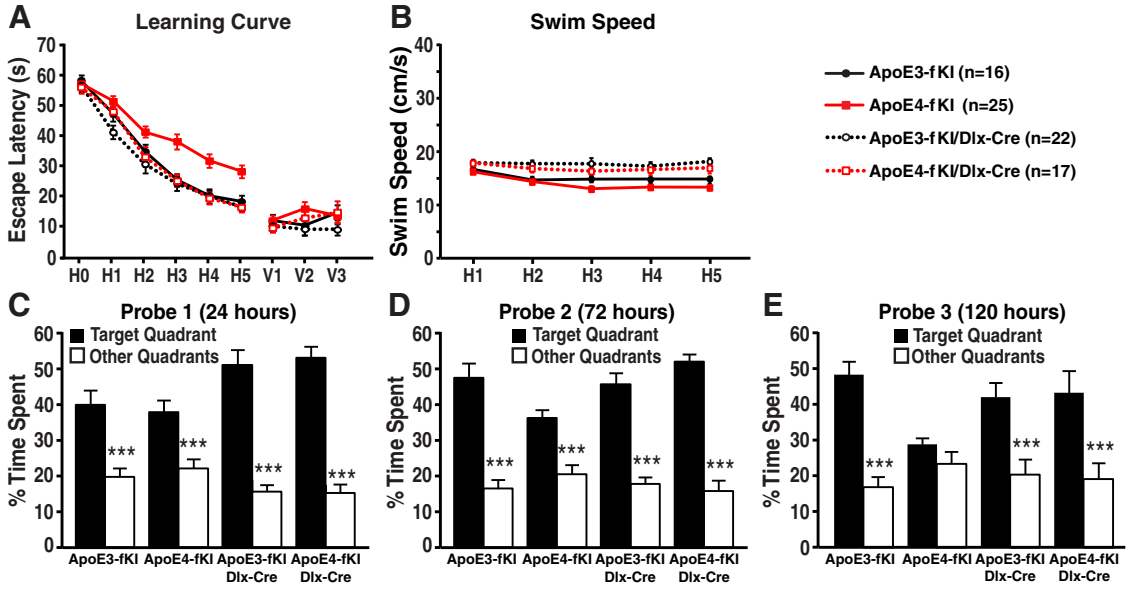

Figure 6. Deletion of apoE4 in GABAergic interneurons was sufficient to prevent the development of spatial learning and memory deficits in aged mice. ***A***, Seventeen-month-old female apoE3-fKI, apoE4-fKI, apoE3-fKI/Dlx-Cre, and apoE4-fKI/Dlx-Cre mice were tested in the MWM. Points represent averages of daily trials. H, hidden platform day (2 trials per session, 2 sessions per day); H0, first trial on H1; V, visible platform day (1 trial per platform location, 3 sessions per day). Escape latency (*y*-axis) indicates time to reach the target. In the hidden platform days, latencies of all groups of mice were analyzed and compared by repeated-measures ANOVA and Bonferroni *post hoc* test. ApoE4-fKI mice learned significantly slower than apoE3-fKI mice ($p < 0.01$). ApoE4-fKI/Dlx-Cre mice learned as well as apoE3-fKI mice ($p > 0.05$), which was significantly faster than apoE4-fKI mice ($p < 0.001$). There was no significant difference between apoE3-fKI and apoE3-fKI/Dlx-Cre mice. ***B***, Swim speed was similar among the four groups of mice. ***C–E***, Probe 1, 2, and 3 trials were performed 24, 72, and 120 h, respectively, after the last day of hidden platform training. Percentage time spent in the target quadrant versus the average percentage time spent in other three quadrants was compared for each group of mice. ***$p < 0.001$ (one-way ANOVA and Bonferroni *post hoc* test).

aim to understand the neural and behavior deficits affected by apoE4 expression in different types of brain cells under physiologic expression levels. Previous studies relied on transgenic mouse or cell-culture models to study the cellular source-dependent effects of apoE4. Indeed, transgenic mice that express human apoE4 under a GFAP promoter at physiological levels on a mouse *apoe* knock-out background did not have deficits in spatial memory tasks, although they developed a working memory deficit (Hartman et al., 2001). On the other hand, transgenic mice that express apoE4 under a neuron-specific enolase (NSE) promoter on a mouse *apoe* knock-out background had earlier and more severe deficits in spatial memory tasks (Raber et al., 1998).

While apoE is normally highly expressed in astrocytes, deleting apoE4 in these cells does not protect aged mice from apoE4-induced learning and memory deficits. This suggests that astrocytic apoE4 does not contribute significantly to cognitive deficits in mice. In accordance with our findings, astrocytic apoE4 was actually excitoprotective, as shown for astrocytic apoE3, in response to kainic acid treatment of GFAP-apoE transgenic mice. However, neuronal apoE4 resulted in neurodegeneration in NSE-apoE transgenic mice under the same conditions,

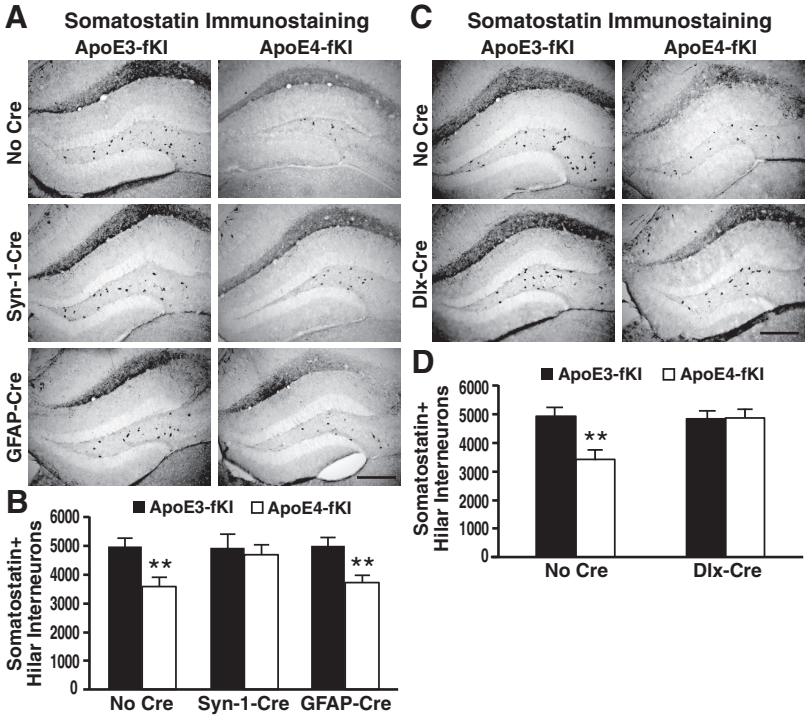

Figure 7. Endogenously produced apoE4 causes loss of somatostatin-positive interneurons. ***A***, Representative images of anti-somatostatin-immunostained sections of the dentate gyrus of 17-month-old female apoE3-fKI, apoE4-fKI, apoE3-fKI/Syn-1-Cre, apoE4-fKI/Syn-1-Cre, apoE3-fKI/GFAP-Cre, and apoE4-fKI/GFAP-Cre mice. Scale bar, 250 μm. ***B***, Quantification of somatostatin-positive hilar interneurons in 17-month-old female apoE3-fKI, apoE4-fKI, apoE3-fKI/Syn-1-Cre, apoE4-fKI/Syn-1-Cre, apoE3-fKI/GFAP-Cre, and apoE4-fKI/GFAP-Cre mice ($n = 8$ for each group of mice). ***C***, Representative images of anti-somatostatin immunostained sections of the dentate gyrus of 17-month-old female apoE3-fKI, apoE4-fKI, apoE3-fKI/Dlx-Cre, and apoE4-fKI/Dlx-Cre mice. Scale bar, 250 μm. ***D***, Quantification of somatostatin-positive hilar interneurons in 17-month-old female apoE3-fKI, apoE4-fKI, apoE3-fKI/Dlx-Cre, and apoE4-fKI/Dlx-Cre mice ($n = 8$ for each group of mice). **$p < 0.01$ (*t* test).

while neuronal apoE3 did not (Buttini et al., 2010). Likewise, neuronal apoE4 decreased dendrite arborization and spine density in NSE-apoE transgenic mice, whereas astrocytic apoE4 did not show similar effects in GFAP-apoE transgenic mice (Jain et al., 2013).

CNS neurons also express apoE, especially in response to stress and injury (Xu et al., 2006; Huang, 2010; Huang and Mucke, 2012). Here, we show that deleting apoE in astrocytes results in ~80% loss of total apoE. The remaining ~20% likely represents neuronal apoE expression, as we found that deleting apoE in neurons leads to ~20% decrease of total apoE levels. Neuronal expression of apoE might represent a mechanism to fight against stresses and injuries (Aoki et al., 2003; Xu et al., 2006; Melemedjian et al., 2013). However, in the context of apoE4, it is preferentially cleaved by an unknown protease in neurons, generating neurotoxic apoE fragments that escape the secretory pathway, enter the cytosol, and cause mitochondrial impairment and tau phosphorylation (Brecht et al., 2004; Chang et al., 2005; Andrews-Zwilling et al., 2010). These detrimental effects of apoE4 eventually lead to neuronal loss, especially hilar GABAergic interneuron loss, contributing to AD pathogenesis (Huang and Mucke, 2012).

The GABAergic system plays an important role in cognition, particularly in learning and memory (Castellano et al., 1993; Collinson et al., 2002; Andrews-Zwilling et al., 2012). Dysfunction of the GABAergic system with alterations in GABA or somatostatin levels was clinically associated with dementia, such as AD (Zimmer et al., 1984; Hardy et al., 1987; Seidl et al., 2001), which was accelerated by apoE4 (Grouselle et al., 1998). Additionally, aging—the most evident risk factor for AD—leads to a decrease in GABA levels in the CNS of humans (Bareggi et al., 1982). Studies in wild-type rats and diversity outbred mice similarly show an age-dependent decrease of hilar GABAergic interneurons, especially somatostatin-positive interneurons, which is correlated with learning and memory decline (Spiegel et al., 2013; Koh et al., 2014).

Our current study supports the hypothesis that apoE4 expression in GABAergic interneurons results in inhibitory interneuron loss in the hippocampal hilus, leading to learning and memory deficits (Huang and Mucke, 2012). The loss of inhibitory balance may lead to excitotoxicity and eventually cognitive dysfunction, as also seen in transgenic mice expressing mutant human APP (Palop et al., 2007; Roberson et al., 2011; Verret et al., 2012). It should be noted that, in the current study, the apoE-fKI/Dlx-Cre mice have a loss of apoE in all GABAergic interneurons (not just hilar interneurons). Thus, the prevention of hilar interneuron loss may reflect a direct effect of lacking apoE4 production in hilar interneurons or a network effect of general improvement of interneuron functions. Nevertheless, our data suggest that inhibiting apoE4 expression in GABAergic interneurons and treatments that strengthen hilar GABAergic interneuron function and survival might represent an effective strategy for treating AD. In support of this notion, we have recently demonstrated that hilar transplantation of inhibitory interneuron progenitors restores normal cognitive function in aged apoE4-KI mice without or with amyloid-β accumulation (Tong et al., 2014).

References

Andrews-Zwilling Y, Bien-Ly N, Xu Q, Li G, Bernardo A, Yoon SY, Zwilling D, Yan TX, Chen L, Huang Y (2010) Apolipoprotein E4 causes age- and Tau-dependent impairment of GABAergic interneurons, leading to learning and memory deficits in mice. J Neurosci 30:13707–13717. CrossRef Medline

Andrews-Zwilling Y, Gillespie AK, Kravitz AV, Nelson AB, Devidze N, Lo I, Yoon SY, Bien-Ly N, Ring K, Zwilling D, Potter GB, Rubenstein JL, Kreitzer AC, Huang Y (2012) Hilar GABAergic interneuron activity controls spatial learning and memory retrieval. PLoS One 7:e40555. CrossRef Medline

Aoki K, Uchihara T, Sanjo N, Nakamura A, Ikeda K, Tsuchiya K, Wakayama Y (2003) Increased expression of neuronal apolipoprotein E in human brain with cerebral infarction. Stroke 34:875–880. CrossRef Medline

Bajenaru ML, Zhu Y, Hedrick NM, Donahoe J, Parada LF, Gutmann DH (2002) Astrocyte-specific inactivation of the neurofibromatosis 1 gene (NF1) is insufficient for astrocytoma formation. Mol Cell Biol 22:5100–5113. CrossRef Medline

Bareggi SR, Franceschi M, Bonini L, Zecca L, Smirne S (1982) Decreased CSF concentrations of homovanillic acid and gamma-amino butyric acid in Alzheimer's disease. Age- or disease-related modifications? Arch Neurol 39:709–712. CrossRef Medline

Bien-Ly N, Gillespie AK, Walker D, Yoon SY, Huang Y (2012) Reducing human apolipoprotein E levels attenuates age-dependent Abeta accumulation in mutant human amyloid precursor protein transgenic mice. J Neurosci 32:4803–4811. CrossRef Medline

Brecht WJ, Harris FM, Chang S, Tesseur I, Yu GQ, Xu Q, Fish JD, Wyss-Coray T, Buttini M, Mucke L, Mahley RW, Huang Y (2004) Neuron-specific apolipoprotein E4 proteolysis is associated with increased tau phosphorylation in brains of transgenic mice. J Neurosci 24:2527–2534. Medline

Buttini M, Masliah E, Yu GQ, Palop JJ, Chang S, Bernardo A, Lin C, Wyss-Coray T, Huang Y, Mucke L (2010) Cellular source of apolipoprotein E4 determines neuronal susceptibility to excitotoxic injury in transgenic mice. Am J Pathol 177:563–569. CrossRef Medline

Caselli RJ, Dueck AC, Osborne D, Sabbagh MN, Connor DJ, Ahern GL, Baxter LC, Rapcsak SZ, Shi J, Woodruff BK, Locke DE, Snyder CH, Alexander GE, Rademakers R, Reiman EM (2009) Longitudinal modeling of age-related memory decline and the APOE ε4 effect. N Engl J Med 361:255–263. CrossRef Medline

Castellano C, Introini-Collison IB, McGaugh JL (1993) Interaction of beta-endorphin and GABAergic drugs in the regulation of memory storage. Behav Neural Biol 60:123–128. CrossRef Medline

Chang S, Ma T, Miranda RD, Balestra ME, Mahley RW, Huang Y (2005) Lipid- and receptor-binding regions of apolipoprotein E4 fragments act in concert to cause mitochondrial dysfunction and neurotoxicity. Proc Natl Acad Sci U S A 102:18694–18699. CrossRef Medline

Collinson N, Kuenzi FM, Jarolimek W, Maubach KA, Cothliff R, Sur C, Smith A, Otu FM, Howell O, Atack JR, McKernan RM, Seabrook GR, Dawson GR, Whiting PJ, Rosahl TW (2002) Enhanced learning and memory and altered GABAergic synaptic transmission in mice lacking the alpha 5 subunit of the GABAA receptor. J Neurosci 22:5572–5580. Medline

Corder EH, Saunders AM, Strittmatter WJ, Schmechel DE, Gaskell PC, Small GW, Roses AD, Haines JL, Pericak-Vance MA (1993) Gene dose of apolipoprotein E type 4 allele and the risk of Alzheimer's disease in late onset families. Science 261:921–923. CrossRef Medline

De Jager PL, Shulman JM, Chibnik LB, Keenan BT, Raj T, Wilson RS, Yu L, Leurgans SE, Tran D, Aubin C, Biffi A, Corneveaux JJ, Huentelman MJ, Rosand J, Daly MJ, Myers AJ, Reiman EM, Bennett DA, Evans DA (2012) A genome-wide scan for common variants affect in the rate of age-related cognitive decline. Neurobiol Aging 33:1017.e1–1017.e15. CrossRef Medline

Farrer LA, Cupples LA, Haines JL, Hyman B, Kukull WA, Mayeux R, Myers RH, Pericak-Vance MA, Risch N, van Duijn CM (1997) Effects of age, sex, and ethnicity on the association between apolipoprotein E genotype and Alzheimer disease. A meta-analysis. APOE and Alzheimer Disease Meta Analysis Consortium. JAMA 278:1349–1356. CrossRef Medline

Gallagher M, Burwell R, Burchinal M (1993) Severity of spatial learning impairment in aging: development of a learning index for performance in the Morris water maze. Behav Neurosci 107:618–626. CrossRef Medline

Grouselle D, Winsky-Sommerer R, David JP, Delacourte A, Dournaud P, Epelbaum J (1998) Loss of somatostatin-like immunoreactivity in the frontal cortex of Alzheimer patients carrying the apolipoprotein epsilon 4 allele. Neurosci Lett 255:21–24. CrossRef Medline

Hardy J, Selkoe DJ (2002) The amyloid hypothesis of Alzheimer's disease: progress and problems on the road to therapeutics. Science 297:353–356. CrossRef Medline

Hardy J, Cowburn R, Barton A, Reynolds G, Dodd P, Wester P, O'Carroll AM, Lofdahl E, Winblad B (1987) A disorder of cortical GABAergic innervation in Alzheimer's disease. Neurosci Lett 73:192–196. CrossRef Medline

Harris FM, Brecht WJ, Xu Q, Tesseur I, Kekonius L, Wyss-Coray T, Fish JD, Masliah E, Hopkins PC, Scearce-Levie K, Weisgraber KH, Mucke L, Mah-

ley RW, Huang Y (2003) Carboxyl-terminal-truncated apolipoprotein E4 causes Alzheimer's disease-like neurodegeneration and behavioral deficits in transgenic mice. Proc Natl Acad Sci U S A 100:10966–10971. CrossRef Medline

Hartman RE, Wozniak DF, Nardi A, Olney JW, Sartorius L, Holtzman DM (2001) Behavioral phenotyping of GFAP-apoE3 and GFAP-apoE4 transgenic mice: apoE4 mice show profound working memory impairments in the absence of Alzheimer's-like neuropathology. Exp Neurol 170:326–344. CrossRef Medline

Huang Y (2010) Abeta-independent roles of apolipoprotein E4 in the pathogenesis of Alzheimer's disease. Trends Mol Med 16:287–294. CrossRef Medline

Huang Y, Mucke L (2012) Alzheimer mechanisms and therapeutic strategies. Cell 148:1204–1222. CrossRef Medline

Jain S, Yoon SY, Leung L, Knoferle J, Huang Y (2013) Cellular source-specific effects of apolipoprotein (apo) E4 on dendrite arborization and dendritic spine development. PLoS One 8:e59478. CrossRef Medline

Keenan BT, Shulman JM, Chibnik LB, Raj T, Tran D, Sabuncu MR, Alzheimer's Disease Neuroimaging Initiative, Allen AN, Corneveaux JJ, Hardy JA, Huentelman MJ, Lemere CA, Myers AJ, Nicholson-Weller A, Reiman EM, Evans DA, Bennett DA, De Jager PL (2012) A coding variant in CR1 interacts with APOE-epsilon4 to influence cognitive decline. Hum Mol Genet 21:2377–2388. CrossRef Medline

Koh MT, Spiegel AM, Gallagher M (2014) Age-associated changes in hippocampal-dependent cognition in diversity outbred mice. Hippocampus. Advance online publication. doi:10.1002/hipo.22311. CrossRef

Lambert JC, Ibrahim-Verbaas CA, Harold D, Naj AC, Sims R, Bellenguez C, DeStafano AL, Bis JC, Beecham GW, Grenier-Boley B, Russo G, Thorton-Wells TA, Jones N, Smith AV, Chouraki V, Thomas C, Ikram MA, Zelenika D, Vardarajan BN, Kamatani Y, et al. (2013) Meta-analysis of 74,046 individuals identifies 11 new susceptibility loci for Alzheimer's disease. Nat Genet 45:1452–1458. CrossRef Medline

Leung L, Andrews-Zwilling Y, Yoon SY, Jain S, Ring K, Dai J, Wang MM, Tong L, Walker D, Huang Y (2012) Apolipoprotein E4 causes age- and sex-dependent impairments of hilar GABAergic interneurons and learning and memory deficits in mice. PLoS One 7:e53569. CrossRef Medline

Løkkegaard A, Nyengaard JR, West MJ (2001) Stereological estimates of number and length of capillaries in subdivisions of the human hippocampal region. Hippocampus 11:726–740. CrossRef Medline

Madisen L, Zwingman TA, Sunkin SM, Oh SW, Zariwala HA, Gu H, Ng LL, Palmiter RD, Hawrylycz MJ, Jones AR, Lein ES, Zeng H (2010) A robust and high-throughput Cre reporting and characterization system for the whole mouse brain. Nat Neurosci 13:133–140. CrossRef Medline

Maei HR, Zaslavsky K, Wang AH, Yiu AP, Teixeira CM, Josselyn SA, Frankland PW (2009) What is the most sensitive measure of water maze probe test performance? Front Integr Neurosci 3:33. CrossRef Medline

Mahley RW, Huang Y (2012) Apolipoprotein E sets the stage: response to injury triggers neuropathology. Neuron 76:871–885. CrossRef Medline

Melemedjian OK, Yassine HN, Shy A, Price TJ (2013) Proteomic and functional annotation analysis of injured peripheral nerves reveals ApoE as a protein upregulated by injury that is modulated by metformin treatment. Mol Pain 9:14. CrossRef Medline

Mouton PR, Gokhale AM, Ward NL, West MJ (2002) Stereological length estimation using spherical probes. J Microsc 206:54–64. CrossRef Medline

Palop JJ, Chin J, Roberson ED, Wang J, Thwin MT, Bien-Ly N, Yoo J, Ho KO, Yu GQ, Kreitzer A, Finkbeiner S, Noebels JL, Mucke L (2007) Aberrant excitatory neuronal activity and compensatory remodeling of inhibitory hippocampal circuits in mouse models of Alzheimer's disease. Neuron 55:697–711. CrossRef Medline

Perrin RJ, Fagan AM, Holtzman DM (2009) Multimodal techniques for diagnosis and prognosis of Alzheimer's disease. Nature 461:916–922. CrossRef Medline

Potter GB, Petryniak MA, Shevchenko E, McKinsey GL, Ekker M, Rubenstein JL (2009) Generation of Cre-transgenic mice using Dlx1/Dlx2 enhancers and their characterization in GABAergic interneurons. Mol Cell Neurosci 40:167–186. CrossRef Medline

Raber J, Wong D, Buttini M, Orth M, Bellosta S, Pitas RE, Mahley RW, Mucke L (1998) Isoform-specific effects of human apolipoprotein E on brain function revealed in ApoE knock-out mice: increased susceptibility of females. Proc Natl Acad Sci U S A 95:10914–10919. CrossRef Medline

Ramos B, Baglietto-Vargas D, del Rio JC, Moreno-Gonzalez I, Santa-Maria C, Jimenez S, Caballero C, Lopez-Tellez JF, Khan ZU, Ruano D, Gutierrez A, Vitorica J (2006) Early neuropathology of somatostatin/NPY GABAergic cells in the hippocampus of a PS1xAPP transgenic model of Alzheimer's disease. Neurobiol Aging 27:1658–1672. CrossRef Medline

Rempe D, Vangeison G, Hamilton J, Li Y, Jepson M, Federoff HJ (2006) Synapsin I Cre transgene expression in male mice produces germline recombination in progeny. Genesis 44:9–44. CrossRef

Roberson ED, Halabisky B, Yoo JW, Yao J, Chin J, Yan F, Wu T, Hamto P, Devidze N, Yu GQ, Palop JJ, Noebels JL, Mucke L (2011) Amyloid-beta/Fyn-induced synaptic, network, and cognitive impairments depend on tau levels in multiple mouse models of Alzheimer's disease. J Neurosci 31:700–711. CrossRef Medline

Saunders AM, Strittmatter WJ, Schmechel D, George-Hyslop PH, Pericak-Vance MA, Joo SH, Rosi BL, Gusella JF, Crapper-MacLachlan DR, Alberts MJ (1993) Association of apolipoprotein E allele epsilon 4 with late-onset familial and sporadic Alzheimer's disease. Neurology 43:1467–1472. CrossRef Medline

Seidl R, Cairns N, Singewald N, Kaehler ST, Lubec G (2001) Differences between GABA levels in Alzheimer's disease and Down syndrome with Alzheimer-like neuropathology. Naunyn Schmiedebergs Arch Pharmacol 363:139–145. CrossRef Medline

Shi H, Belbin O, Medway C, Brown K, Kalsheker N, Carrasquillo M, Proitsi P, Powell J, Lovestone S, Goate A, Younkin S, Passmore P, Morgan K (2012) Genetic variants influencing human aging from late-onset Alzheimer's disease (LOAD) genome-wide association studies (GWAS). Neurobiol Aging 33:1849.e5–1849.e18. CrossRef Medline

Spiegel AM, Koh MT, Vogt NM, Rapp PR, Gallagher M (2013) Hilar interneuron vulnerability distinguishes aged rats with memory impairment. J Comp Neurol 521:3508–3523. CrossRef Medline

Strittmatter WJ, Weisgraber KH, Huang DY, Dong LM, Salvesen GS, Pericak-Vance M, Schmechel D, Saunders AM, Goldgaber D, Roses AD (1993) Binding of human apolipoprotein E to synthetic amyloid beta peptide: isoform-specific effects and implications for late-onset Alzheimer disease. Proc Natl Acad Sci U S A 90:8098–8102. CrossRef Medline

Takahashi H, Brasnjevic I, Rutten BP, Van Der Kolk N, Perl DP, Bouras C, Steinbusch HW, Schmitz C, Hof PR, Dickstein DL (2010) Hippocampal interneuron loss in an APP/PS1 double mutant mouse and in Alzheimer's disease. Brain Struct Funct 214:145–160. CrossRef Medline

Tong LM, Djukic B, Arnold C, Gillespie AK, Yoon SY, Wang MM, Zhang O, Knoferle J, Rubenstein JL, Alvarez-Buylla A, Huang Y (2014) Inhibitory interneuron progenitor transplantation restores normal learning and memory in apoE4 knock-in mice without or with Aβ accumulation. J Neurosci 34:9506–9515. CrossRef Medline

Uhlmann EJ, Wong M, Baldwin RL, Bajenaru ML, Onda H, Kwiatkowski DJ, Yamada K, Gutmann DH (2002) Astrocyte-specific TSC1 conditional knockout mice exhibit abnormal neuronal organization and seizures. Ann Neurol 52:285–296. CrossRef Medline

Verret L, Mann EO, Hang GB, Barth AM, Cobos I, Ho K, Devidze N, Masliah E, Kreitzer AC, Mody I, Mucke L, Palop JJ (2012) Inhibitory interneuron deficit links altered network activity and cognitive dysfunction in Alzheimer model. Cell 149:708–721. CrossRef Medline

West MJ (1993) Regionally specific loss of neurons in the aging human hippocampus. Neurobiol Aging 14:287–293. CrossRef Medline

Xu Q, Bernardo A, Walker D, Kanegawa T, Mahley RW, Huang Y (2006) Profile and regulation of apolipoprotein E (ApoE) expression in the CNS in mice with targeting of green fluorescent protein gene to the ApoE locus. J Neurosci 26:4985–4994. CrossRef Medline

Zhang B, Gaiteri C, Bodea LG, Wang Z, McElwee J, Podtelezhnikov AA, Zhang C, Xie T, Tran L, Dobrin R, Fluder E, Clurman B, Melquist S, Narayanan M, Suver C, Shah H, Mahajan M, Gillis T, Mysore J, MacDonald ME, et al. (2013) Integrated systems approach identifies genetic nodes and networks in late-onset Alzheimer's disease. Cell 153:707–720. CrossRef Medline

Zhu Y, Romero MI, Ghosh P, Ye Z, Charnay P, Rushing EJ, Marth JD, Parada LF (2001) Ablation of NF1 function in neurons induces abnormal development of cerebral cortex and reactive gliosis in the brain. Genes Dev 15:859–876. CrossRef Medline

Zimmer R, Teelken AW, Trieling WB, Weber W, Weihmayr T, Lauter H (1984) Gamma-amino butyric acid and homovanillic acid concentration in the CSF of patients with senile dementia of Alzheimer's type. Arch Neurol 41:602–604. CrossRef Medline